

RESEARCH PAPER

Novel Pure Aluminium Silicate Nono Particles As Remenirazing Fillers for Dental Light Cured Composite: Synthesis and Physicomechanical Properties

Rafid M. AlBadr¹, Hasanen A. AlNamel^{2*}, Majed Mohamed Refaat²

¹ Department of basic sciences, College of Dentistry, University of Basrah, Basrah, Iraq

² Department of Prosthodontics Dentistry, College of Dentistry, University of Basrah, Basrah, Iraq

ARTICLE INFO

Article History:

Received 24 September 2024

Accepted 18 December 2024

Published 01 January 2025

Keywords:

Compression strength

Flexural Strength

Fracture toughness

Kaolinite

Nanocomposites

Void content test

ABSTRACT

This study aimed to assess how the physical and mechanical properties of dental composites are influenced by the characteristics of natural material fillers. We focused on analyzing the filler properties (using XRD, FTIR, SEM, BET, and density) of a selection of glass materials to identify correlations with their physico-mechanical properties and to evaluate the validity of the current classification system. Filler particles measuring less than 500 nm were extracted from five different composites. The surfaces of these fillers were modified with silane before being mixed with a Bis-GMA/TEGDMA (70/30%) resin. We evaluated the physico-mechanical properties of the tested composites, including depth of cure, void content, flexural strength, compressive strength, and fracture toughness. The average size of the fillers was consistently below 1 μm . Flexural strength values ranged from 70.56 to 110.81 MPa. Due to the solid ceramic characteristics of Aluminiumsilicate, certain mechanical properties, like compressibility, may experience a slight increase as the amount of Aluminiumsilicate decreases.

How to cite this article

AlBadr R., AlNamel H., Refaat M. Novel Pure Aluminium Silicate Nono Particles As Remenirazing Fillers for Dental Light Cured Composite: Synthesis and Physicomechanical Properties J Nanostruct, 2025; 15(1):266-275. DOI: 10.22052/JNS.2025.01.026

INTRODUCTION

In order to restore lost tooth structure, dental caries can be treated using a variety of techniques. While invasive procedures entail the removal and replacement of damaged tooth structure with dental restorations, non-invasive techniques aim to stop active non-cavitated carious lesions [1]. Significant developments in dental resin composites over the last 20 years have led to a high level of stability in both their mechanical and cosmetic qualities [2]. Composites dental filling of Resin-based are increasingly utilized for restoration of the tooth due to several advantages over

traditional restorative materials, including superior aesthetics, cost-effectiveness, and enhanced physical and wear properties [3]. The classification of dental composites has significantly advanced over the years, traditionally emphasizing filler-size distribution, filler content, or composition. Initially, materials were categorized as micro fills and nano fills, which contained only micro or nanoparticles. However, most contemporary resin composites are classified under the hybrid category, more specifically as nanohybrids. This nomenclature is used to describe materials that consist of a mixture of nanoparticles and submicron particles [4].

* Corresponding Author Email: hasanen.muhsen@uobasrah.edu.iq



Inorganic fillers are incorporated into the chemical structure of resin-matrix composites to enhance mechanical properties and to closely replicate the optical characteristics of enamel and dentin [5],[6],[7]. During light curing procedures, these inorganic fillers must facilitate the transmission of visible light necessary for activating the polymerization reaction within the polymeric matrix

The fundamental crystal layer unit of kaolinite, a typical layered silicate clay mineral, is created when SiO tetrahedrons and Al-(O, OH) octahedrons are connected by shared oxygen atoms. [8]. This mineral exhibit stable physical and chemical properties, a high crystalline content, a high specific surface area, effective adsorption capabilities, and does not contribute to secondary pollution. As a result, it is extensively utilized as a carrier material for photocatalysts [8], [9].

The physical and chemical qualities of the filler surface have a significant impact on the mechanical, physical, and biological aspects of the interaction between fillers and the resin matrix. As a result, it is crucial to carefully consider how surface alteration affects the interfacial characteristics. [10], [11].

Over the past decade, extensive research has been conducted on dental resins, fillers, and their interfacial interactions to enhance the performance of dental resin composites and lower production costs [12] However, the complexities surrounding regulation, validation, and product assurance in biomedical materials create significant barriers for new technologies, often delaying their transition to production. Additionally, factors such as the characteristics of biological interfaces, individual patient considerations, and the long-term effects on the durability of restorations can prolong

the demonstration of efficacy [13]. In this study, selected kaolinite, a layered clay mineral that does not swell in water and has a density of 2.78 g/cm³. The interlamellar space can be expanded to the required size for nanoparticle synthesis by disrupting the hydrogen bonds that tightly connect the kaolinite layers.

This study explored the potential of utilizing low-cost natural materials, such as nano aluminum silicate, found in the environment for applications in dentistry, particularly in light-cured composites. The null hypotheses proposed were: (1) Following the combustion of the aluminum silicate nanoparticles along with other inorganic compounds to create the fillers, the nanoparticles will persist. (2) The physical and mechanical properties of the dental composites will remain unchanged, with no enhancements observed in their characteristics.

MATERIALS AND METHODS

Preparation of Ca-Si-Al-O-Na-F Glasses

Kaolinite (Al₂O₇Si₂-2H₂O or Al₂O₃·2SiO₂·2H₂O) used in this study was supplied by Sigma Eldritch German company as a source of aluminum silicate (Si-Al) material. CaF₂ (99%, UNI- Chem), NaF (99%, MERCK), A total of 100g of glass components, including Kaolinite, Calcium Fluoride (CaF₂), P₂O₅ and CaO Prepared from oyster shells and diagnosed in our laboratories [14], were weighed in specific ratios to prepare five groups with varying compositions, as detailed in Table 1. After two hours of processing in a ball mill, the mixture was sieved to remove any particles larger than 75µm. In order to create glass, the resultant mixture was heated for two hours from room temperature to 1200°C in an electric furnace (Ivoclar Vivadent Programat P500, Germany) at a rate of 5°C per

Table 1. The compositions of the glass fillers (%wt.) prepared for tested composites.

Group of glass	ka	CaO	P2O5	CaF	NaF
Ka_oys 0%	80	0	6	9	5
Ka_oys 10%	70	10	6	9	5
Ka_oys 20%	60	20	6	9	5
Ka_oys 30%	50	30	6	9	5
Ka_oys 40%	40	40	6	9	5

minute from 50 to 500°C and 10°C per minute from 500 to 1200°C. Following this heating time, the glass was subjected to rapid cooling. To obtain a powder for further examination, the resultant glass was first crushed for two more hours in a ball mill (RETSCH PM 100, Germany) and then sieved through a mesh with an aperture of less than 25 µm.

Characterization of Glasses

To identify the crystalline phases and ascertain whether the materials were amorphous or crystalline, X-ray diffraction analysis was employed. High-magnification pictures of the sample glass and its crystallization zones were taken using a scanning electron microscope (SEM). This close-up image was helpful in understanding the crystallizations process. The SEM (VEGA TESCAN, Czech) was used to describe the glass samples' size and morphology. CCl₄ is used as an immersion liquid with an uncertainty of ± 0.02 g/cm³ in order to determine the density using the buoyancy method, which is based on the Archimedean principle.

A Philips Powder Diffractometer fitted with a copper (Cu K) X-ray source (Philips PW 1700 series, Leiden, Netherlands) was used to perform X-ray diffraction (XRD). Using a continuous mode with a step size of 0.02 degrees and a counting time of 0.35 seconds per step, the powder samples, which had a particle size of less than 10 µm, were scanned in the 2θ range of 10 to 70 degrees. Powder surface area and porosity are measured using the Brunauer-Emmett-Teller (BET) technique. An inert gas is added in regulated amounts after a sample has first been degassed under heat and vacuum and chilled to the temperature of liquid nitrogen (77K). The gas adsorbs onto the surface and forms a monolayer as the pressure within the sample chamber rises. A second layer of gas can arise because of the dipole this monolayer produces. A CHEMBET 3000 QUANTACHROME apparatus is used to perform the BET analysis, and the adsorption/desorption gas is nitrogen. The formula [Brunauer et al. 1938] is used to determine the mean diameter obtained from the BET technique, represented as d_{BET} : $d_{BET} = 6 / (A_s \rho)$ (2) In this equation, A_s represents the specific surface area (m²/g), and ρ denotes the theoretical density of the phase. The density of the glass is determined using the pycnometric method, with an uncertainty of ± 0.02 g/cm³.

Composite preparation

In order to initiate and crosslink the composite, catalysts such as camphor Quinone (CQ, Aldrich (UK)) and dimethylaminoethylmethacrylate (DMAEMA, Wako Pure Chemical Industries) were added to the resin, which had a composition of BisGMA (Sigma Aldrich (UK))/TEGDMA (Sigma Aldrich (UK)) with a w%/w% ratio of 70/30. Ten series of the prepared light activated composites were tested. In our lab, we synthesized and sintered calcium fluoroaluminosilicate glass using a previously described method [17]. The particles' average size was within 1.2µm. Following treatment of these particles, γ-methacryloxypropyltrimethoxy (γMPS) silane (Aldrich (UK) 440159) was utilized as a silane-coupling agent and added at 76 weight percent to the resin. Table 1 displays the components of the dental composites under study.

The diluent monomer, TEGDMA (Tokyo Chemical Industry, Japan), was combined with the monomer resins Bis-GMA (Tokyo Chemical Industry, Japan) at a weight percentage ratio of 70:30. To ensure that all of the ingredients are well distributed, this mixture is now stirred for roughly two hours. An hour is spent mixing the concoction once all the ingredients have been added. To prevent premature polymerization, light exposure should be avoided at this stage. To polymerize the resin matrix, an LED Light Curing Unit (550 mW/cm²) was used. For 40 seconds, light was used to cure the samples with varying weight percentages of filler particles (Table 1).

Physical and mechanical properties

All composite materials' depth of cure (DOC) was evaluated after the scratching process specified in ISO 4049:2019 (Dentistry, 2019). At least three samples, each measuring 4 mm in diameter and 8 mm in thickness, were made and polymerized from one side. Any uncured material was then scraped off using a spatula. A caliper with a precision of ±0.01 mm was used to measure the thickness of the cured composites at four distinct locations. The DOC was calculated by averaging and halving the values derived from these measurements.

Void content test

The void content of the samples was determined by comparing theoretical density with apparent density. The theoretical density of the samples

was calculated using the Eq. 1 [16]:

$$\rho_{th} = \frac{W_1 + W_2 + W_3 + W_4 + W_5}{\frac{W_1}{\rho_1} + \frac{W_2}{\rho_2} + \frac{W_3}{\rho_3} + \frac{W_4}{\rho_4} + \frac{W_5}{\rho_5}} \quad (1)$$

where $\rho_1, \rho_2, \rho_3, \rho_4,$ and ρ_5 represent the densities of various materials.

The apparent densities of the samples were obtained using the pycnometric method. Subsequently, the void content for each sample was calculated.

Using the 3-point bending method and a universal testing equipment (STM-20, Santam, Iran) with a cross-head speed of 1 mm/min, the samples' flexural strength was assessed. Bar specimens that were 2 mm 2 mm 25 mm in size were made in accordance with ISO 4049 guidelines. The specimens were exposed to a light-

curing unit (Opti lux 501, Kerr, USA) at an intensity of 550 (mwt/cm²) for 200 seconds on each side. The samples were submerged in distilled water at 37°C for a full day before testing. The following formula was then used to calculate the flexural strength (FS) in MPa (Eq. 2) [17]:

$$FS (MPa) = \frac{3pL}{2bd^2} \quad (2)$$

In this context, P represents the load at fracture measured in newtons (N). The symbol L denotes the span length, fixed at 20 mm. The variables b and d correspond to the width and thickness of the specimens, respectively, both expressed in millimeters. The compressive strength of the examined composites was assessed through standardized testing. Five cylindrical specimens were fabricated using stainless steel molds with dimensions of 4.0 mm in diameter and 6.0 mm in

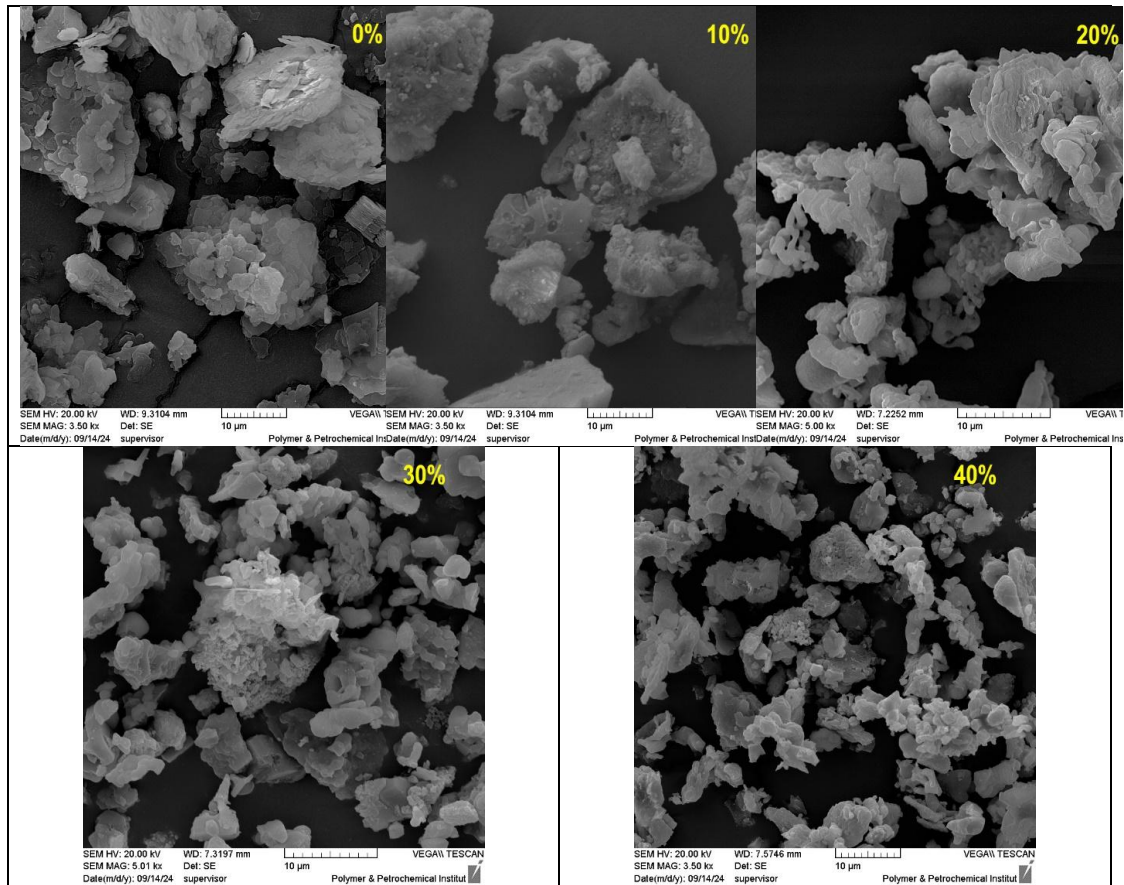


Fig. 1. The SEM spectra of experimental glasses..

height, adhering to the stipulations set forth by ISO 9917-1:2007. These specimens underwent light curing for a duration of 40 seconds. Subsequently, the cured specimens were submerged in deionized water maintained at a temperature of 37°C for a period of 24 hours. The tests were conducted using a universal mechanical testing machine (Zwick/Roell, 2020, Germany) equipped with a 2

kN load cell, operating at a speed of 0.5 mm/min⁻¹ (Eq. 3) [18].

$$CS (Mpa) = \frac{4F}{\pi D^2} \quad (3)$$

where F is the maximum load in N, and D (mm) is the diameter of the specimen in mm

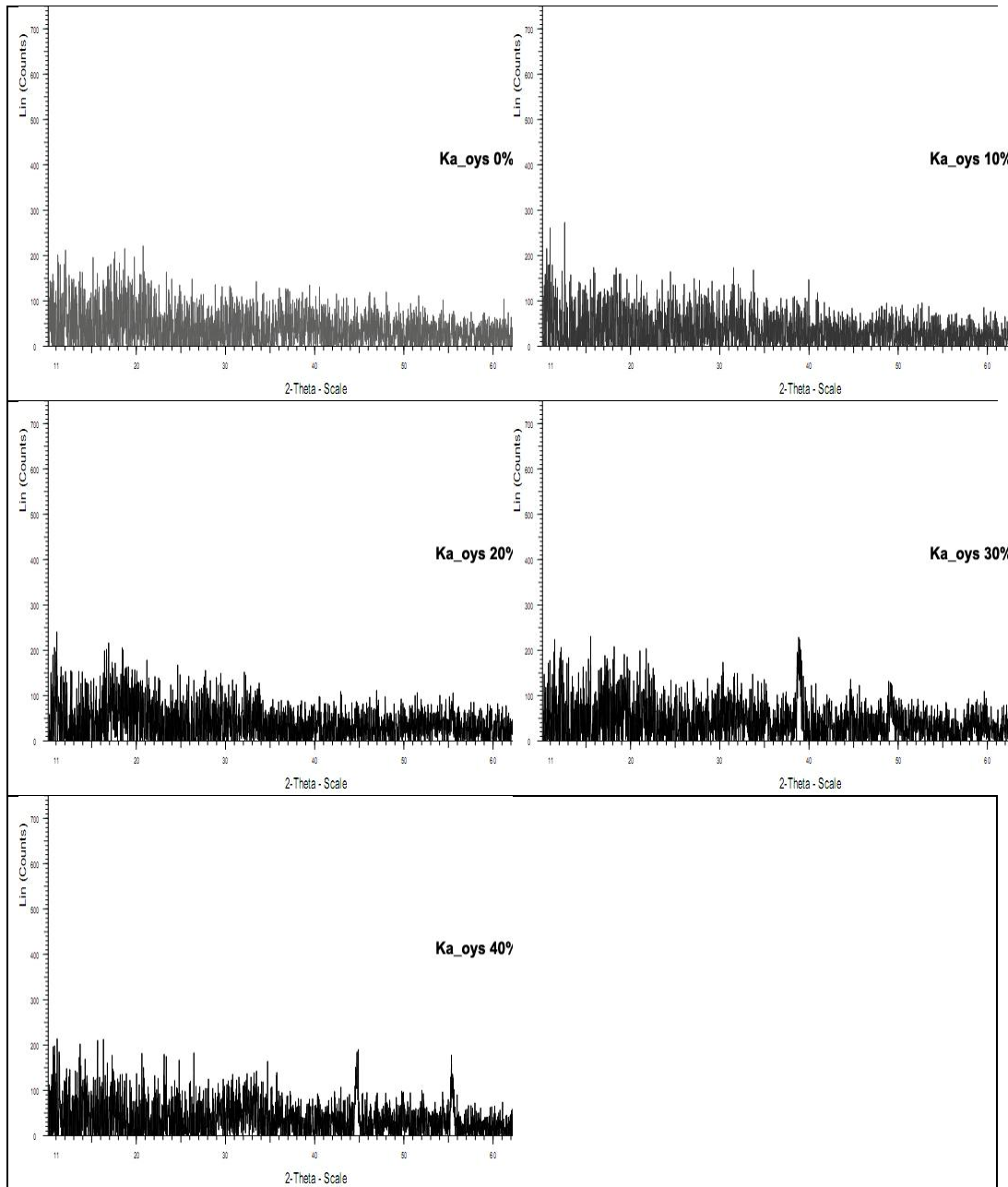


Fig. 2. the XRD patterns of experimental glasses.

The stress intensity factor (K) during crack propagation determines a material's fracture toughness. Single-edge notch beam (SENB) specimens were made in compliance with ASTM Standard E399-90 in order to evaluate fracture toughness (FT). A 2.5 mm center notch was made

with a razor blade to construct these specimens in a 5 mm × 2 mm x 25 mm split steel mould. A universal testing machine was used to perform the bending fracture test at a cross-head speed of 0.1 mm/min. The critical stress intensity factor (K_{IC}), which is a measure of fracture toughness, was

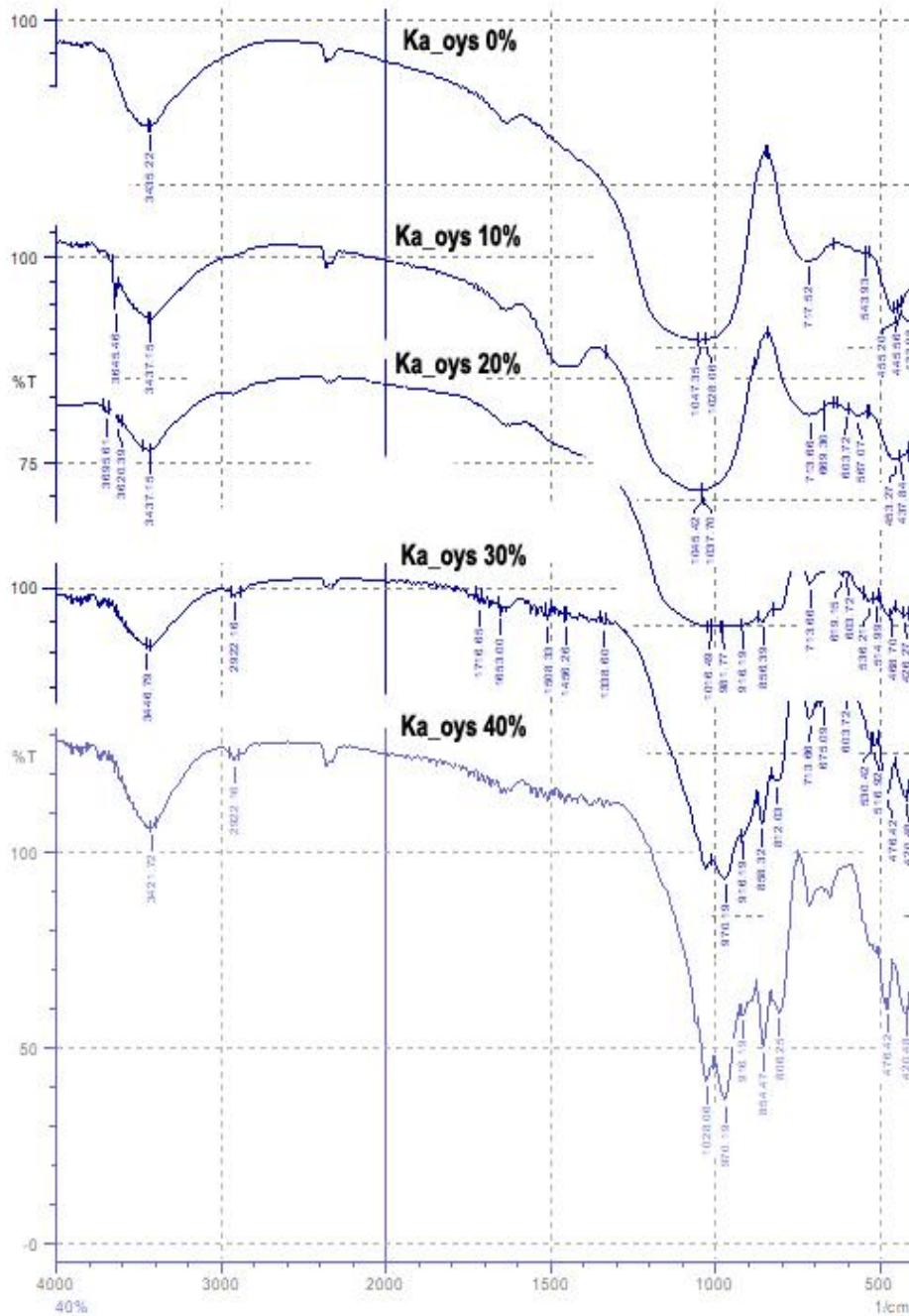


Fig. 3. The FTIR spectra of experimental glasses.

$$K_{IC} = \frac{3PL}{2BW^{3/2}} \{1.93\alpha^{1/2} - 3.07\alpha^{3/2} + 14.53\alpha^{5/2} - 25.11\alpha^{7/2} + 25.8\alpha^{9/2}\} \quad (4)$$

then determined using the Eq. 4.

P stands for the load at the fracture site in Newtons in this case. The specimen’s length, breadth, thickness, and notch length all expressed in millimeters are represented by the variables L, W, B, and a. The experiment used a span length of 20 mm and a load cell capacity of 60 N. Mode I crack opening, denoted by the subscript IC, happens when a normal tensile stress is applied perpendicular to the fracture plane.

RESULTS AND DISCUSSION

SEM analysis showed distinct morphologies for the micro and fillers (Fig. 1), ranging from spherical to rough and irregular particles. With the exception of the material containing relatively large fillers (Ka_ows 0%), the irregular particles exhibited varying degrees of sharpness in their shapes. In terms of particle size, the largest particles measured in the tens of microns across several materials, while in others, the largest did not exceed 1 µm. Additionally, very fine particles, approximately 100 nm in size, were also observed.

XRD patterns of experimental glasses (Fig. 2) displays patterns reveal that the peaks corresponding to the crystalline phases are

superimposed on the broad band’s characteristic of the amorphous glass phase. Notably, the samples with 10% and 20% Ka_ows are entirely vitreous, while the sample with 30% Ka_ows exhibits peaks at 2θ values of 31° and 59°. Additionally, there are some low-intensity peaks that could not be identified. However, these extra peaks in both systems do not significantly affect the glass characteristics of the materials.

Sio’s bending vibration mode. The symmetric stretching vibration of Si–O and the straight, asymmetric stretching vibration of Si–O–Si bridges are represented by additional peaks at 875 cm⁻¹ and 1099 cm⁻¹, respectively. At around 450 cm⁻¹, the O–Al peak is visible. The existence of Si–O–Si and Al–O–Si bonds, which are essential parts of the GIC samples’ lattice and vulnerable to acid attack—a process required to create dental compounds—is confirmed by this research. Furthermore, P–O vibrations are responsible for the peaks at 530 and 620 cm⁻¹ that appear in all spectra. [14]. A peak at 555 cm⁻¹, which corresponds to the bending vibrations of the PO4 structure, indicates the existence of phosphate inside the glass structure. Furthermore, a high Ca²⁺ concentration causes a band to develop at 1432 cm⁻¹ (Fig. 3). [19].

Table 2. Density, crystalline size and particles size for experimental glass.

experimental glass	Surface area (m ² /g)	density (g/cm ³)	d _(BET) µm	Crystal size nm
Ka_ows 0%	7.88	2.42	0.31	24.947
Ka_ows 10%	8.06	2.54	0.29	27.078
Ka_ows 20%	8.53	2.59	0.27	25.334
Ka_ows 30%	8.75	2.69	0.25	22.362
Ka_ows 40%	8.93	2.88	0.23	24.486

Table 3. Depth of cure in (mm) and Void contents (%) for experimental composites.

experimental composites	DC (mm)	Theoretical density (g/cm ³)	Void contents (%)
Ka_ows 0%	3.33 (0.06)	1.905413	3.941663
Ka_ows 10%	3.35 (0.05)	1.962241	3.149537
Ka_ows 20%	3.37 (0.17)	1.986195	2.933391
Ka_ows 30%	3.38 (0.11)	2.02949	0.854624
Ka_ows 40%	3.41 (0.007)	2.107054	1.192725



Table 3 displays the average depth of cure for the experimental composites. The depth of cure for the Ka_0ys 40% and Ka_0ys 0% composites was measured at 3.33 ± 0.06 mm and 3.38 ± 0.11 mm, respectively. No significant differences were observed among these four groups. However, the depth of cure for the Ka_0ys 40% composite was significantly greater than that of the other composites.

As detailed in the methodology section, the void content of various samples was calculated. The results of the void content tests for the specimens are shown in Table 3. The analysis of these results indicates a significant decrease in void content with an increase in CaO loading. This trend aligns

well with findings from previous studies [12]. The observed reduction in void content can be attributed to the smaller particle size and the spacing between adjacent filler particles. An increase in filler correlates with a higher void content, as illustrated in Table 2.

In terms of flexural properties, as shown in Table 3, it was noted that strength increased steadily with the addition of CaO. However, samples containing 40% CaO experienced a significant drop in strength upon the addition of the additive, and strength levels remained relatively stable at higher filler concentrations. Typical flexural stress-strain curves for the prepared composites are illustrated in Fig. 4.

Table 4. The results for compressive strength.

examined Composites	N=5		
	Flexural strength (MPa)	Compressive strength (MPa)	Fracture toughness (MPa.m ^{3/2})
Ka_0ys 0%	70.56 (6.46)	218.02 (13.59)	1.14 (0.07)
Ka_0ys 10%	81.59 (6.29)	220.33 (10.98)	1.31 (0.10)
Ka_0ys 20%	88.37 (10.51)	231.73 (14.98)	1.36 (0.11)
Ka_0ys 30%	110.81 (3.28)	246.92 (11.29)	1.57 (0.14)
Ka_0ys 40%	76.49 (8.57)	221.53 (9.82)	1.23 (0.06)

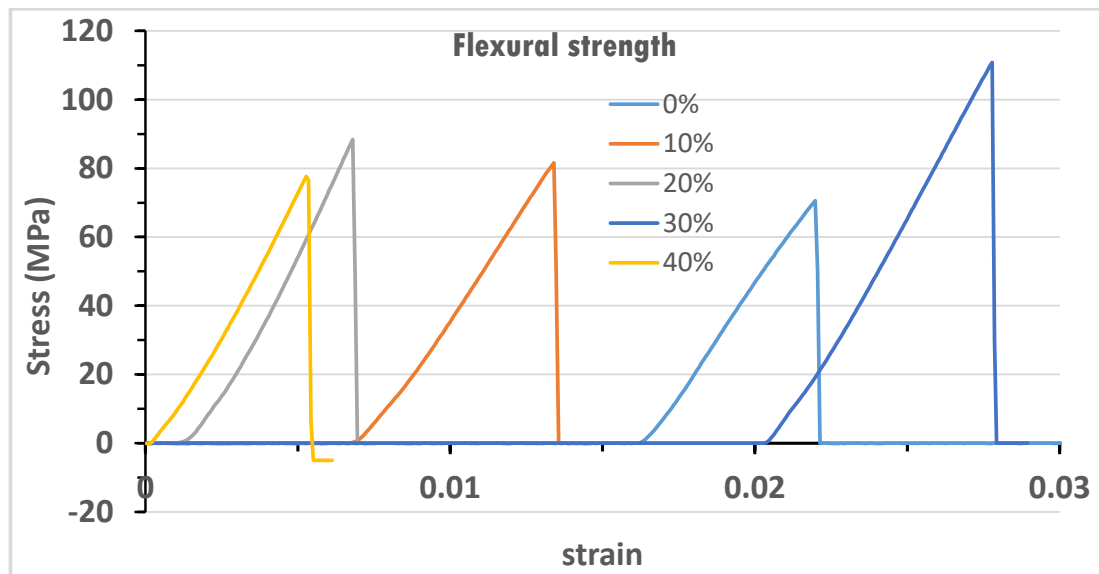


Fig. 4. Flexural strain-stress plot describes yielding point in the examined composites.

The results for compressive strength are presented in Table 4. The composite with 30% CaO (Ka_0ys) exhibited the highest compressive strength, measuring 246 ± 11 MPa. In contrast, the compressive strength values for the composites with 0%, 10%, and 40% CaO were approximately 220 MPa. Nevertheless, the average compressive strength for these samples remains notably high.

Fracture toughness (K_{IC}) values, along with their standard deviations, are summarized in Table 2. The KIC values ranged from 1.14 (± 0.07) to 1.57 (± 0.14) MPa/m^{0.5}. Among the materials tested, Ka_0ys 30% demonstrated the highest mean fracture toughness, significantly outperforming all other composite materials in this study. In contrast, Ka_0ys 0% had the lowest mean fracture toughness, which was significantly inferior compared to the rest. In addition, no significant differences were observed between the mean fracture toughness values of the laboratory-processed Ka_0ys 10% and Ka_0ys 20% composites.

To improve the qualities of bioactive glasses, it is essential to understand the structure. The alkali metal concentration and its function within the structure are intimately related to a number of physical properties, such as transition temperature, softening point, and solubility. Therefore, our comprehension of the relationship between structure and characteristics will be greatly enhanced by obtaining a greater grasp of the structural role of the alkali metal component.

Recent simulations indicate that, although significantly less common than Si-O-Si linkages, Si-P bridges are present in bioactive glasses, and their prevalence rises with higher phosphate concentrations. It is well-established that Si-P copolymerization can occur in silicate glasses and melts. The introduction of P₂O₅ into a pure silica melt does not result in the depolymerization of the silicate network; instead, it facilitates the substitution of phosphorus within the network.

Fluormica glass-ceramic has the following qualities: good machinability, moderate thermal expansion, great translucency, strong chemical resistance, hardness similar to genuine teeth, and good flexural strength (around 150 MPa). 55% of its volume is made up of tiny, block-like tetra silicic Fluormica platelets of the floral glass type, which are 1-2 μ m in size and 0.5 μ m thick.

In clinical practice, achieving close contact between the light cure unit and the tooth surface during posterior restorations can be

challenging, making the depth of cure a critical factor. This aspect can significantly influence the overall success of the restoration. Inadequate polymerization within the restoration may lead to clinical issues such as marginal leakage, pulpal inflammation, and ultimately, restoration failure [20]. In the current study, the depth of cure values obtained using the ISO 4049 method were notably higher for the Ka_0ys 40% composite compared to the other experimental composites. The high translucency of the Ka_0ys 40% composite contributes to its enhanced depth of cure.

As detailed in the methodology section, the void content of various samples was calculated. The results of the void content tests for the specimens are shown in Table 3. The analysis of these results indicates a significant increase in void content with higher filler loading. This trend aligns well with findings from previous studies [12]. The increase in void content can be attributed to the spacing between adjacent filler particles; as the amount of filler increases, so does the void content (see Table 4).

Flexural strength are key tests used to evaluate the mechanical properties of polymer-based composites. These assessments help determine the ability of restorative materials to withstand the flexural stresses encountered during the chewing process. According to the ISO 4049 standard, the minimum flexural strength required for occlusal tooth surface restoration is 74.2 MPa, while for other teeth, it is set at 50 MPa. According to experimental data, adding SiO fillers to the created dental composite improves its flexural strength and modulus (see Table 2). The Ka_0ys 30% composites showed a greater flexural strength of 110.81 MPa, whereas the Ka_0ys 0% composites had the lowest flexural strength, measuring 70.56 MPa. The existence of more harder ceramic particles, which add intrinsic hardness and stiffness and eventually make the composite more brittle, may be the cause of the observed loss in flexural strength for the Ka_0ys 40% composites, even with the higher SiO filler. [21].

Because it acts as a bridge between opposing teeth and restorative composite materials, the compressive strength of dental restoratives is essential to the chewing process. According to experimental data, the produced dental composite's compressive strength rose to 246.92 MPa when 30% CaO fillers were added (for Ka_0ys), but it fell to 221.53 MPa when 40% CaO

fillers were added. Effective interfacial bonding between the resin matrix and the 30% CaO filler is responsible for the first increase in compressive strength for Bioglass-filled composites. The 30% Ka_oys fillers' increased crosslinking density inside the polymer matrix, which improves the mechanical qualities of the dental composites, is probably the cause of this strong binding. Effective load transmission is made possible by adding hard, rigid filler particles to a polymer matrix, which increases the stiffness and strength of the comparatively soft and weak matrix. In various clinical trials involving multiple composite systems, the fracture toughness of the core composite correlates strongly with clinical outcomes. This relationship was considered when developing a new classification system for composites, which is now included in the international standard ISO 16586:2000 (International Organization for Standardization) based on established clinical indications.

CONCLUSION

The study's experimental findings show that when the proportion of Kaolinite filler by weight in the dental composite declined, so did the void content. Kaolinite helps to boost the dental composite's compressive strength since it is a ceramic substance with a significant amount of stiffness.

CONFLICT OF INTEREST

The authors declare that there is no conflict of interests regarding the publication of this manuscript.

REFERENCES

- Schwendicke F, Walsh T, Lamont T, Al-Yaseen W, Bjørndal L, Clarkson JE, et al. Interventions for treating cavitated or dentine carious lesions. The Cochrane database of systematic reviews. 2021;7(7):CD013039-CD013039.
- Tauböck TT, Jäger F, Attin T. Polymerization shrinkage and shrinkage force kinetics of high- and low-viscosity dimethacrylate- and ormocer-based bulk-fill resin composites. *Odontology*. 2018;107(1):103-110.
- Yadav R, Kumar M. Dental restorative composite materials: A review. *J Oral Biosci*. 2019;61(2):78-83.
- Ferracane JL. Resin composite—State of the art. *Dent Mater*. 2011;27(1):29-38.
- Habib E, Wang R, Zhu XX. Monodisperse silica-filled composite restoratives mechanical and light transmission properties. *Dent Mater*. 2017;33(3):280-287.
- Alnamel HA, Abdul Baqi HJ. Assessment of the Effects of

- Boron Nitride Nanoplatelets Reinforcement on the Physical and Mechanical Properties of the Geopolymer Prepared by Natural Kaolinite: An In Vitro Study. *Dent Hypotheses*. 2024;15(1):11-13.
- Habib E, Wang R, Wang Y, Zhu M, Zhu XX. Inorganic Fillers for Dental Resin Composites: Present and Future. *ACS Biomaterials Science & Engineering*. 2015;2(1):1-11.
- Cao Z, Wang Q, Cheng H. Recent advances in kaolinite-based material for photocatalysts. *Chin Chem Lett*. 2021;32(9):2617-2628.
- Cheng H, Liu Q, Xu P, Hao R. A comparison of molecular structure and de-intercalation kinetics of kaolinite/quaternary ammonium salt and alkylamine intercalation compounds. *J Solid State Chem*. 2018;268:36-44.
- Chen M, Yang T, Han J, Zhang Y, Zhao L, Zhao J, et al. The Application of Mineral Kaolinite for Environment Decontamination: A Review. *Catalysts*. 2023;13(1):123.
- Xu X, He L, Zhu B, Li J, Li J. Advances in polymeric materials for dental applications. *Polymer Chemistry*. 2017;8(5):807-823.
- Makvandi P, Gu JT, Zare EN, Ashtari B, Moeini A, Tay FR, et al. Polymeric and inorganic nanoscopic antimicrobial fillers in dentistry. *Acta Biomater*. 2020;101:69-101.
- AlBadr RM, Halfi SA, Ziadan KM. The effectiveness of oyster filler on the physical and mechanical properties of novel dental restorative composite. *AIP Conference Proceedings: AIP Publishing*; 2020. p. 050001.
- Cho K, Rajan G, Farrar P, Prentice L, Prusty BG. Dental resin composites: A review on materials to product realizations. *Composites Part B: Engineering*. 2022;230:109495.
- Thbayh KK, AlBadr RM, Ziadan KM, Thbayh DK, Mohi SM, Fiser B. Fabrication and characterization of novel glass-ionomer cement prepared from oyster shells. *Sci Rep*. 2024;14(1):24083-24083.
- Aljaberi K, M. AlBadr R, M. Ziadan K. A new approach to prepare nano hydroxyapatite from oyster shells used for dental applications. *Journal of Kufa-Physics*. 2022;14(02):35-46.
- Saini S, Yadav R, Sonwal S, Meena A, Huh YS, Brambilla E, et al. Tribological, mechanical, and thermal properties of nano tricalcium phosphate and silver particulates reinforced Bis-GMA/TEGDMA dental resin composites. *Tribology International*. 2024;199:110010.
- AlNamel H, M. AlBadr R, Abdul Razzaq F. Evaluation and Characterization of some Properties of Glass Ionomer Cement Reinforced by Novel Boron Nitride Nanoplatelets. *Frontiers in Biomedical Technologies*. 2024.
- Thadathil Varghese J, Raju R, Farrar P, Prentice L, Prusty BG. Comparative analysis of self-cure and dual cure-dental composites on their physico-mechanical behaviour. *Aust Dent J*. 2023;69(2):124-138.
- Fousekis E, Lolis A, Marinakis E, Oikonomou E, Foros P, Koletsi D, et al. Short fiber-reinforced composite resins as post-and-core materials for endodontically treated teeth: A systematic review and meta-analysis of in vitro studies. *The Journal of Prosthetic Dentistry*. 2023.
- Yadav S, Gangwar S. The effectiveness of functionalized nano-hydroxyapatite filler on the physical and mechanical properties of novel dental restorative composite. *International Journal of Polymeric Materials and Polymeric Biomaterials*. 2019;69(14):907-918.